

# **Material Microstructure Effects in Micro-Endmilling of Cu99.9E**

**A.M. Elkaseer<sup>1,2</sup>, S.S. Dimov<sup>3</sup>, D.T. Pham<sup>4</sup>, K.P. Popov<sup>5</sup>, L. Olejnik<sup>6</sup> and A. Rosochowski<sup>7</sup>**

<sup>1</sup>*IK4-TEKNIKER, c/Iñaki Goenaga 5, Eibar, Guipuzcoa, Spain*

<sup>2</sup>*Department of Production Engineering & Mechanical Design, Faculty of Engineering, Port Said University, Port Said, 42523, Egypt*

<sup>3,4</sup>*Department of Mechanical Engineering, University of Birmingham, Birmingham, B15 2TT, UK*

<sup>5</sup>*Faculty of Computing, Engineering and Science, University of South Wales, Pontypridd, CF37 1DL, UK*

<sup>6</sup>*Institute of Manufacturing Techniques, Warsaw University of Technology – Narbutta 85, 02-524 Warsaw, Poland*

<sup>7</sup>*Design, Manufacture and Engineering Management, University of Strathclyde – 75 Montrose Street, Glasgow G1 1XJ, United Kingdom*

## **Abstract**

This paper presents an investigation of the machining response of materials metallurgically and mechanically modified at the micro-scale. Tests were conducted that involved micro-milling slots in coarse-grained (CG) Cu99.9E with an average grain size of 30  $\mu\text{m}$  and ultrafine-grained (UFG) Cu99.9E with an average grain size of 200 nm, produced by Equal-Channel Angular Pressing (ECAP).

A new method based on Atomic Force Microscope (AFM) measurements is proposed for assessing materials' microstructure effects in micro machining, i.e. the effects of material homogeneity changes on the minimum chip thickness required for a robust micro cutting processes with a minimum surface roughness.

The investigation has shown that by refining the material microstructure the minimum chip thickness can be reduced and a high surface finish can be obtained. Also, conclusions were made that material homogeneity improvements lead to a reduction in surface roughness and surface defects in micro-cutting.

Keywords: micro-endmilling, material microstructure, grain size effects, surface finish, surface defects, ECAP, AFM, minimum chip thickness.

## **1. Introduction**

For some time there has been an accelerating trend for products to be made smaller; this is particularly true in avionics, biotechnology, communications, electronics and medicine [1-9]. The technical complexity and the broad range of requirements that such miniaturised devices have to satisfy means that the manufacturing methods used for their production should be able to process different materials, including aluminium alloys, brass, ceramics, composites, copper, plastics, stainless steel and titanium [1, 9]. There are stringent requirements on both the micro fabrication techniques and materials used because of the need for reliable and robust components [10].

A number of micro-manufacturing technologies have been developed for producing micro products/components. Among these techniques manufacturing methods that produce micro-features by removing material from a workpiece have shown high potential [8]. Different material removal mechanisms can be employed but predominantly mechanical and energy-based processes are used, i.e. mechanical micro-machining,  $\mu$ -laser ablation and  $\mu$ -EDM [1-5, 8]. In addition, new bio-enabled techniques have been recently proposed that utilise microorganisms and bacteria to

remove undesirable material from workpieces in a controllable manner [11-12]. They offer some advantages over other available technologies, i.e. low-energy consumption, no thermal damage and production of complex shapes, however the technology is still at its early stages of development and needs more optimisation to achieve higher material removal rates and improve the obtainable surface quality [12].

Presently, micro-milling is the most popular machining technology when complex 3-D microstructures are required [13] due to its accuracy, cost effectiveness, flexibility, and surface finish that can be achieved. However, important differences exist between micro- and macro-scale machining which have a significant influence on the material removal mechanisms [1]. This is because the grain sizes of most commonly used engineering materials, such as aluminium, copper and steel, and the feature sizes of micro-machined components or the edge radius of the cutting tools can be comparable in scale, as shown in Fig. 1, and therefore the material cannot be considered anymore isotropic or fully homogeneous [1, 5]. Consequently, it is necessary to carry out sub-grain size (mechanical) processing [14]. Additionally, the crystalline texture of the material resulting from its processing could lead to variations in chip thickness and therefore the machining process can be considered to some extent stochastic. Cutting takes place in the so-called dislocation micro-crack range and the thickness of the removed material varies from 10  $\mu\text{m}$  to 100 nm [14]. In particular, the cutting process of micro-scale machining does not rely only on developing micro-cracks along the grain boundaries but also involves dislocation slips in the crystalline structure of the material. In addition, during cutting, the dislocation density increases due to dislocations' multiplication and the formation of new ones. Thus, material microstructure effects are important in micro-machining [1], and the specific processing energy required to initiate

chip formation depends directly on the ability of a given metal to produce dislocation slips [14].

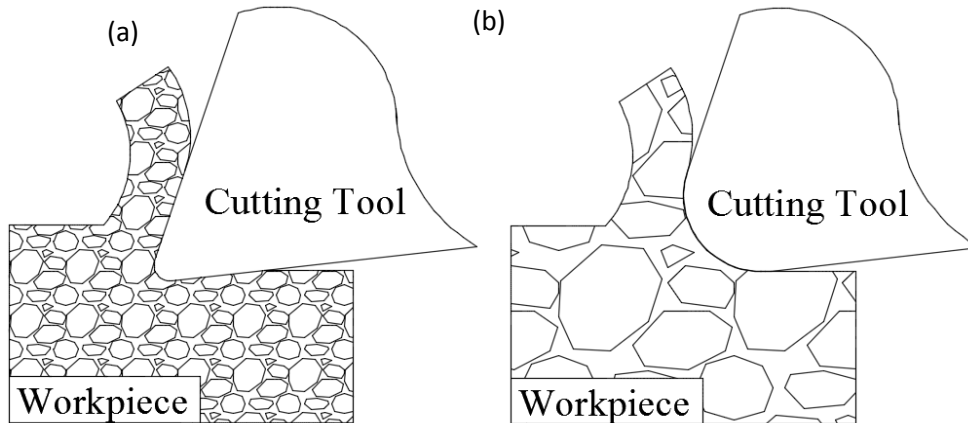


**Fig. 1: (a) macro and (b) micro cutting, showing relative dimensions of cutting tool and grain size**

This paper reports on a series of micro-milling experiments under different conditions to investigate the machining response of metallurgically and mechanically modified Cu99.9E workpieces with coarse and ultrafine grained microstructures. The aim was to determine the effects of material microstructure on machining conditions and surface quality.

In addition, a high-precision method of assessing the homogeneity of the material microstructure is proposed based on Atomic Force Microscope (AFM) measurements of the coefficient of friction. This method offers a comparative assessment of the modified microstructure which enables initial prediction of the minimum chip thickness required to avoid detrimental changes in the cutting conditions. The results of machining two Cu99.9E workpieces with different microstructures are presented and the material effects on the surface quality are analysed and discussed.

Following a review of related research, the remainder of the paper is organised as follows. First, the workpiece materials used in the research are discussed. Then, a method to assess the microstructure effects on materials' homogeneity based on AFM measurements is presented. Next, the machining conditions used in the experiments are described and the rationale behind their selection is explained. Finally, the results from the carried out investigation of the material microstructure effects on cutting mechanisms and surface quality are discussed. Conclusions are made about the influence of material microstructure and cutting conditions on surface quality and also about the effectiveness of the proposed method for assessing the homogeneity of the workpiece material.

## **2. Literature review**

The achievable surface finish is one of the most important characteristics of any machining process. In micro-endmilling, the roughness of the machined surface can be of the same order as the dimensions of the functional features and the resulting surface finish is very difficult and almost impossible to improve by follow up post processing. The roughness generated in micro-scale machining cannot be fully explained using only kinematic parameters because surface effects play an important part in the process. It has been shown that the most important factors that affect the cutting mechanism are the tool cutting edge radius and properties of the workpiece material, particularly heterogeneity, grain size, elastic recovery and strain-hardening effects [15, 16].

### **2.1. Process parameters effects**

Jiao and Cheng [17] examined the outcomes of different milling strategies using CVD diamond ball micro-endmills in terms of resulting surface quality on polymethyl

methacrylate workpieces. The micro-milling strategy included tilting the tool, giving it either a lean angle of  $5^\circ$  or  $15^\circ$ , or a lead angle of  $15^\circ$ . This was done to prevent the occurrence of zero cutting speed and associated rubbing at the ball point. Results showed that lower surface roughness was achieved when the feed and cutting directions were perpendicular to each other. Furthermore significant improvements were achieved by introducing a two-way machining strategy with up- and down-milling. However, optimum results, i.e. a roughness of 8.72 nm, were obtained when the two-way strategy was combined with a lean angle of  $5^\circ$  and a Z-stepover of 1  $\mu\text{m}$  but this was limited to only a small machining area in the experiments due to the process dynamics.

Llanos *et al.*, [18] conducted experimental studies on micro-milling of thin walls using tungsten carbide micro-end milling tools and thus to produce features with high aspect ratios. Two test materials were used, i.e. aluminium and brass. The tests conducted on both materials showed that down-milling gave a lower surface roughness than up-milling. Both materials provided better surface finish with higher spindle speeds. The axial depth of cut did not have any significant effect on the resulting surface finish and also the effect of the axial depth of cut was not linear. The minimum mean roughness was obtained at the lower settings of the axial depth of cut and feed rate and the higher spindle speed.

Kuram and Ozcelik [19] carried out an experimental study with the aim of optimising micro-milling parameters for Ti6Al4V titanium alloy and inconel 718 superalloy, both of which are widely used in the aerospace industry. Using analysis of variance the relative percentage contributions of micro-milling parameters on cutting forces, surface roughness and tool wear were investigated and regression models were developed. It was stated that these models could be used to predict cutting forces, surface roughness and tool wear in micro-milling of these materials. It was also found

that in micro-milling of Ti6Al4V, surface roughness and Peak-to-Valley (P-to-V) Fy forces were mainly influenced by spindle speed, while for Inconel 718, the most effective parameter was feed rate. Also, it was reported that surface roughness and tool wear in micro-milling of Ti6Al4V and Inconel 718 were highly dependent on cutting conditions.

## 2.2. Material microstructure effect

Furukawa and Moronuki [20] observed different cutting mechanisms for polycrystalline, single crystal and amorphous materials, and also for brittle and ductile materials. They recommended that, by increasing the undeformed chip thickness to ten times the average grain size for a given material, it would be possible to avoid the negative crystallographic effects of a non-homogeneous material microstructure.

Uhlmann *et al.*, [21] reported an experimental study into micro-milling of sintered tungsten-copper composite materials with different ratios of tungsten and copper. They pointed out a strong relationship between surface quality and homogeneity of the material microstructure.

Popov *et al.*, [22] investigated the response of mechanically modified Al 5083 alloy when milling thin features of micro components. They showed that through refinement of the material microstructure it was possible to significantly improve the surface integrity of the machined micro features.

Min *et al.*, [23] reported significant variation of surface and edge quality for single-crystal and polycrystalline copper workpieces due to different crystallographic orientations. For polycrystalline materials chip formation is influenced by the microstructure of the material, such as grain boundaries and grain orientation. For single single-crystal materials it is influenced by crystallographic orientation. These

observations confirmed that microstructure variations have a significant effect on the burr topography, resulting surface roughness and edge quality.

Mian *et al.*, [24] experimentally investigated at micro-scale, the machinability of coarse-grained, multi-phase ferrite/pearlite AISI 1040 steel. This material was selected because its typical grain size is large. It was found that the obtained surface roughness was highly dependent on the edge radius of the tool used and material microstructure, especially the grain size. It was concluded that both parameters should be determined prior to the machining operation and thus to optimise cutting conditions and achieving the best possible surface quality.

In subsequent research, Mian *et al.*, [25] experimentally compared two different steels; AISI 1005 (low carbon steel), and AISI 1045 (medium carbon steel with a distinct microstructure of near balance of pearlite and ferrite). The influence of the material microstructure on burr formation, microstructure change, surface finish and tool wear was investigated over a range of chip-loads. In terms of burr formation and tool wear it was found that larger burrs occurred when machining AISI 1005 than when machining AISI 1045, see Fig. 2a and 2b. Chip-load and workpiece material were both found to have a significant influence on the surface roughness. However, the surface finish was found to be more sensitive to chip-load (feed per tooth) and tool edge radius than the grain size of the workpiece material. This was concluded based on the improvements in surface finish obtained for chip-loads numerically close to the tool edge radius. This effect was seen for both workpiece materials (AISI 1005 and AISI 1045) where, despite the differences in material grain sizes, similar roughness values were obtained. Nano-indentation tests were used to characterise the microstructure of the materials and results suggest that this technique could be usefully employed to assess the machinability of different workpieces.

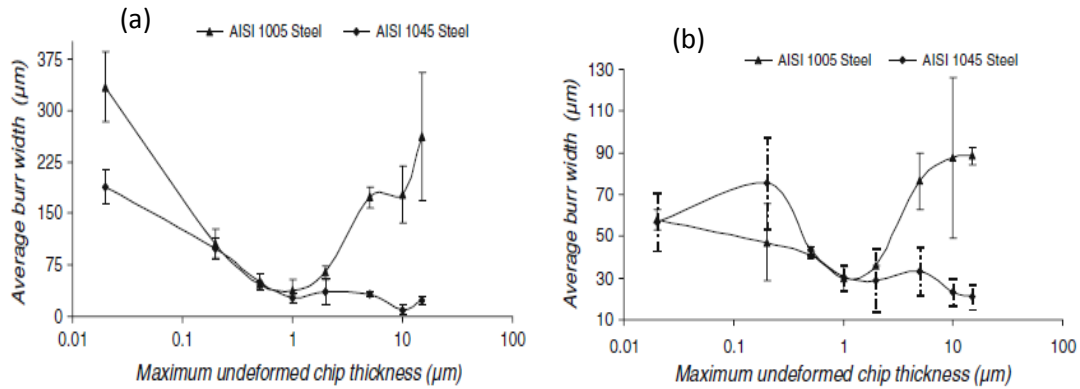


Fig 2: Burr size in (a) down-milling and (b) up-milling [25]

Bajpai *et al.*, [26] investigated the machinability of pyrolytic carbon (PyC), i.e. the interdependences between chip morphology, cutting forces, depth of cut, feed rate, machined surface morphology, spindle speed and surface roughness. Due to the PyC layered anisotropic structure the cutting experiments were carried out parallel to the layers (AB plane) and perpendicular to the layers (C plane). ANOVA analysis was used to identify significant factors that affect the machinability. It was reported that cutting forces were dependent on the used two cutting planes, with an increase of up to 150% when changing from AB to C plane. When cutting in the C plane it was found that any changes of the cutting parameters affected significantly the resulting surface roughness, whereas in the AB plane only tool diameter and feed rate were significant. A conclusion was drawn that the AB plane machining should be preferred because lower cutting forces would be required and a better surface finish could be obtained.

Elkaseer *et al.*, [27] proposed a model to predict the surface roughness generated during micro-endmilling of dual phase materials. The model considered material microstructure together with cutting tool geometry and feed rate. The model was validated in an experimental study, i.e. machining of two different steel samples, AISI 1040 and AISI 8620, under a range of cutting conditions. The authors emphasized that

the model performance was highly dependent on the entered material microstructure and on the use of appropriate cutting conditions.

In follow-up research, Elkaseer *et al.*, [28] developed an analytical model for predicting surface roughness during the micro-machining of multi-phase materials in an experimental setup based on an Atomic Force Microscope (AFM) probe. The model considered the effect of both  $t_{c_{min}}$  and elastic recovery. A series of experimental trials were carried out to validate the model based on scratching CuZn39Pb3, a dual-phase brass alloy, with an AFM-tip. Noticeable differences were observed in regards to the surface roughness obtained on the different phases under the same cutting conditions. This was considered as a clear evidence of the significant material microstructure effects on the resulting roughness in micro/nano cutting of dual-phase materials. The authors claimed good agreement between model and experimental results.

Lauro *et al.*, [29] conducted experimental trials to assess micro-milling forces when machining hardened steel with different grain sizes. It was found that feed rate was the most significant factors affecting the cutting force, i.e. large grain sizes led to lower cutting forces.

In follow-up research, Lauro *et al.*, [30] used an integrated least square model combined with a genetic algorithm to identify the optimal process parameters, i.e. cutting speed, feed rate and grain size were considered. The genetic algorithm was chosen because it is widely considered a robust and efficient optimisation method which can relatively easily be integrated into least squares algorithms. The two main factors considered to optimize micro milling of hardened steel were cutting force and torque. It was found that the most significant parameter in minimising both was the feed rate. However, the results also confirmed that an increase of grain sizes decreases the cutting force and thus affects the responses, particularly when machining hardened steel. The

grain size variation influenced not only the properties of the materials, but also the feature sizes that could be achieved.

The effect of crystallographic orientation when micro-milling a (001) single crystal silicon wafer was studied by Choong *et al.* [31]. White-light interferometry was used to determine edge quality, surface roughness and subsurface residual stress while ANOVA was employed to determine the relative importance of cutting speed, feed rate and axial depth. Up-milling in different directions was carried out using diamond-coated end mills. It was found that machining surfaces along (100) plane were of better quality than those of (110).

### 2.3 Minimum chip thickness in micro-machining

In macro-milling, the chip thickness is sufficiently large and therefore it is not necessary to consider the effects of tool edge radius and uncut chip thickness. One of the important differences between macro- and micro-milling is the reduction in chip thickness which becomes the same order as the cutting edge radius of the tools used and, depending upon the material being milled, the grain size of that material. Researchers in micro-milling often refer to the minimum undeformed thickness of a chip removed from the workpiece surface with a tool with a given cutting edge radius under ideal conditions. This minimum chip thickness ( $t_{c_{min}}$ ) is the cutting limit below which no material removal will occur. It is now known that even a small change in the chip-load can have a significant influence on the material removal mechanism by changing the machining process from cutting to ploughing or slipping. Minimum chip thickness has been investigated by researchers using both analytical and experimental methods [7].

Liu *et al.* [32] developed an analytical model to predict minimum chip thickness ( $t_{c_{min}}$ ) based on slip line theory and consideration of the mechanical and thermal properties of the workpiece and cutting tools under different cutting conditions. However, while a constitutive flow stress model for the processed material is essential for estimating  $t_{c_{min}}$ , few engineering materials have been tested and their constitutive flow stress models derived. It is not yet known whether significant differences in behaviour of modified microstructures is sufficiently small that they follow a similar constitutive flow stress model or whether this approach is limited to standard materials with known characteristics.

Son *et al.*, [33] have proposed an analytical model, Equation 1, to calculate  $t_{c_{min}}$  based on the friction coefficient between the workpiece and the tool and tool edge radius.

$$t_{c_{min}} = r * (1 - \cos(\frac{\pi}{4} - \frac{\beta}{2})) \quad (1)$$

where:  $t_{c_{min}}$  is the minimum chip thickness;

$r$  is the cutting tool edge radius;

$\beta$  is the friction angle between a tool and uncut workpiece.

Mian *et al.*, [34], utilised acoustic emission (AE) to determine the value of  $t_{c_{min}}$  during micro-milling of different workpiece materials. The change of the AE signal were used to identify the threshold conditions for the occurrence of  $t_{c_{min}}$ . The results obtained were in good agreement with published results. The  $t_{c_{min}}$  was found to vary between 11 % and 42 % of the tool edge radius for the used workpiece materials, i.e. AISI 1005 and AISI 1045 steels, Aluminium 6082-T6, Copper (OHFC) and Inconel 718.

Kang *et al.*, [35] investigated how cutting edge radius affected the cutting force and  $t_{c_{min}}$  when micro-milling AISI 1045 steel using tungsten carbide tools. Initial trials were carried out using half-immersion milling to determine the effects of cutting edge radius on the cutting forces. It was found that at lower feeds per tooth, the signals representing the cutting force showed the tool ploughed through and skidded over the surface rather than shearing it. However, when feed per tooth was greater than the cutting edge radius, the micro-scale milling forces appeared similar in form to those in conventional-scale milling processes, where the dominant mechanism is shearing. Cutting force behaviour allowed identification of the uncut  $t_{c_{min}}$ , which was reported to be on average, one third of cutting edge radius of the tool.

Jaffery *et al.*, [36] used ANOVA to analyse performance parameters of a typical micro-machining process, i.e. side burrs, surface roughness and tool wear, to identify key process parameters. It was stated that micro-machining can be classified under two main categories depending on the undeformed chip thickness, particularly when it is greater or less than the tool edge radius. With undeformed chip thickness greater than edge radius, feed rate was the most significant parameter affecting burr width (80% contribution ratio), surface roughness (83%) and tool wear (41%). Thus, this type of machining is closer to macro-machining where the corresponding contributions of feed rate were 75%, 92% and 69%, respectively. When the undeformed chip thickness is less than the tool edge radius, corresponding contributions of feed rate were 52%, 53% and 17%, respectively. These results confirm the importance of tool edge radius and minimum chip thickness in micro-machining.

Oliveira *et al.* [37] investigated size effects in micro- and macro-milling slots in AISI 1045 steel, especially interdependences between cutting force ( $k_c$ ) and chip formation, surface roughness ( $R_a$ ) and tool edge radius ( $r_e$ ). It was reported that feed per

tooth less than the cutting edge radius could lead to a disproportionate increase in the required cutting force and no chip formation. Also, it was found that the minimum uncut chip thickness ranged between 22% and 36% of the endmill edge radius.

He *et al.*, [38] proposed a theoretical model for predicting the size effects on resulting surface roughness in diamond turning when processing fine grain materials. The model considers process kinematics, material spring back, plastic side flow and takes into account certain random factors such vibrations in the workpiece matrix. It was claimed that the copy effect of the tool edge waviness was successfully integrated into the model kinematic element and a minimum undeformed chip thickness related function was derived for determining material spring back. The model's predictions and its experimental validation showed that there was a substantial build-up of unremoved material ahead of the cutting edge when using a diamond cutting tool with large nose radius, and also that the plastic side flow had a greater effect on the resulting surface roughness than the kinematic component. This effect was explained with the inevitable occurrence of an inflection point depending on feed rate that led to size effects on resulting surface roughness.

Willert *et al.*, [39] investigated mechanical loads and surface roughness in precision turning of 42CrMoS4. The focus was on size effects that could occur due to changes in the ratio of undeformed chip thickness to cutting edge radius. It was found that when this ratio was higher than 3 the specific cutting force decreased slowly with its increase while when it was lower than 3 the force increased rapidly with its decrease. Surface roughness showed a similar trend for ratios higher than 3, i.e. it remained more or less constant while for ratios lower than 3, the surface roughness increased rapidly with the decrease of the cutting edge radius.

From the literature review, it is clear that surface roughness and micro features produced by micro-cutting are highly dependent on the material microstructure, especially the material grain size and homogeneity, and the minimum chip thickness of the workpiece material. The motivation for this work was to investigate experimentally the machining response of mechanically and metallurgically modified polycrystalline materials, in particular ultra-fine-grained (UFG) Cu99.9E processed by the ECAP process. For comparison, the machining response of coarse-grained (CG) Cu99.9E was also studied. Another objective was to propose a method for assessing the microstructure effects on the material micro-machining response. In particular, to apply an AFM-based assessment of materials' homogeneity effects on the machining response and thus to be able to select optimal cutting conditions and avoid entering the transitional regime associated with intermittent cutting and ploughing.

### 3. Experimental set-up

This section explains the experimental set-up. First, the microstructures of the workpieces are described. Then, the proposed method of judging the homogeneity of a microstructure is presented. Finally, the selected cutting conditions for the micro-endmilling trials are discussed and the rationale behind their selection is given.

#### 3.1 Workpiece material microstructure

The selected workpiece materials had two different microstructures, a coarse-grained (CG) structure with an average grain size of 30  $\mu\text{m}$  (Figure 3a) and an ultra-fine-grained (UFG) structure with an average grain size of 200 nm (Figure 3b, 3c). The UFG material had been processed by equal channel angular pressing (ECAP) 8 times.

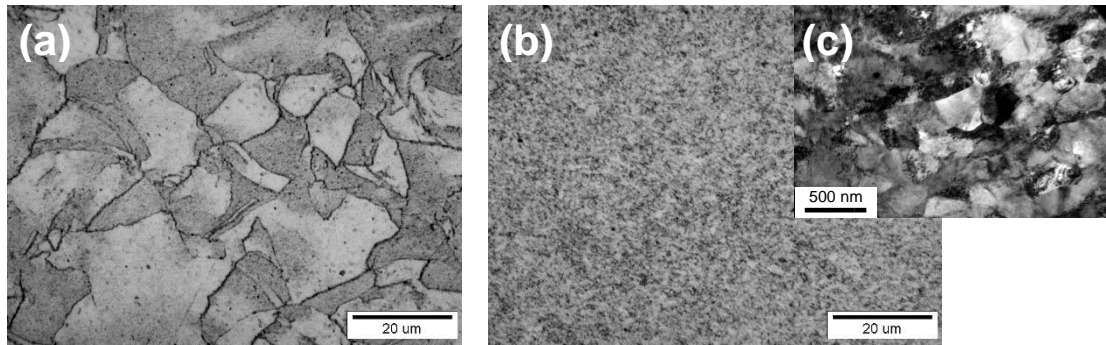


Fig. 3: Microstructure of CG (a) and UFG (b, c) Cu99.9E

### 3.2.1 Material characterisation and minimum chip thickness determination

As previously stated, Son *et al.* [33] proposed an analytical model, Equation 1, to calculate the minimum chip thickness based on the tool edge radius and the friction coefficient between the workpiece and the tool. Generally, there are two methods of obtaining the coefficient of friction and thus the friction angle. One is to conduct a cutting test to measure the ratio of the tangential force and the normal force between the workpiece and the cutting tool [33]. This method requires expensive high-precision equipment (a dynamometer) with a high bandwidth and high sampling frequency capability to provide reliable measurements of the forces generated in micro-milling [2]. As any small amount of noise can give a false cutting force signal, the accurate measurement of very small cutting forces is a challenging issue.

Coefficients of friction between different workpiece materials and cutting tools are reported by researchers [38] but it is unlikely to find the values for any specific material-cutting tool combination. Also, these would be the nominal values of the coefficients of friction that would not be of help for calculating the minimum chip thickness. Therefore, there is a real need for a faster and robust method for measuring the coefficient of friction at the grain scale inside the bulk.

In the research reported here, Son *et al.*'s model was used to calculate the minimum chip thickness. The parallel AFM scan method developed by Bhushan [41], as depicted in Figure 4, was used to calculate the coefficient of friction according to the following equation:

$$\mu = \left( \frac{\Delta W_1 + \Delta W_2}{W_o} \right) * \left( \frac{L}{2 * \ell} \right) \quad (2)$$

where :  $\mu$  is the coefficient of friction;

$\Delta W_1, \Delta W_2$  are the absolute values of changes in the normal force when the sample is travelling along the direction of the cantilever length forward and backward respectively;

$W$  is the applied force between the tip and the sample;  $W$  ranges from 10 to 200 nN;

$L$  is the length of the cantilever;

$\ell$  is the vertical distance between the tip of the cantilever and point P (the fixed point of the cantilever).

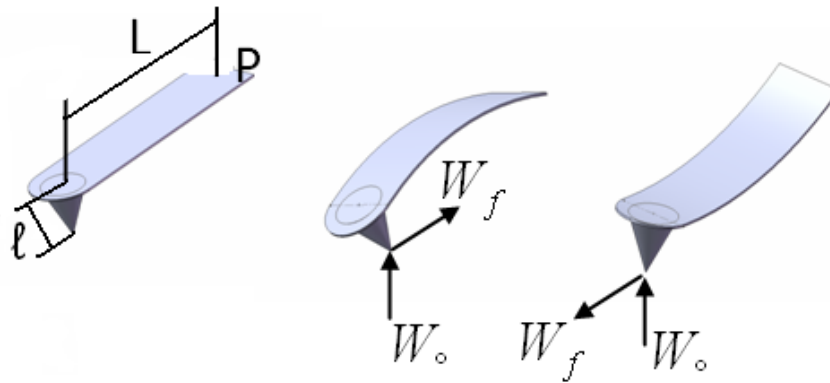


Fig. 4: Friction force in AFM parallel scan

Force measurements were carried out on a XE-100 AFM from Park Systems [42]. Once the coefficient of friction and the cutting edge radius had been determined, the

normalised minimum chip thickness ( $\lambda_n$ ) was calculated;  $\lambda_n$  is the minimum chip thickness divided by the tool edge radius and is a material dependent characteristic [32].

Figure 5 shows how the coefficient of friction varied over the AFM measurement range for both UFG and CG Cu. The average values of UFG and CG Cu were calculated to be 0.46 and 0.35, respectively. Accordingly, when  $r$  equals 2.5  $\mu\text{m}$ , the calculated average minimum chip thickness was 0.39  $\mu\text{m}$  with standard deviation ( $\sigma$ ) = 0.039 for UFG Cu99.9E and 0.48  $\mu\text{m}$  with standard deviation ( $\sigma$ ) = 0.094 for CG Cu99.9E while the normalised minimum chip thickness was 0.156 for UFG Cu and 0.192 for CG Cu (Figure 6). This means that the cutting process started earlier in the case of the UFG Cu sample than for the CG workpiece, and thus a better surface quality would be expected after machining. Also, due to the significant variations in the minimum chip thickness over the scan area for the CG sample, the cutting process would be unstable and would result in highly fragmented chips and defects in the machined surfaces [40]. Conversely, the high homogeneity of the UFG Cu samples results in much less variation in the coefficient of friction and hence in the minimum chip thickness over the scanned area. Therefore the cutting process would be expected to be more stable and the defects on the machined surfaces to decrease.

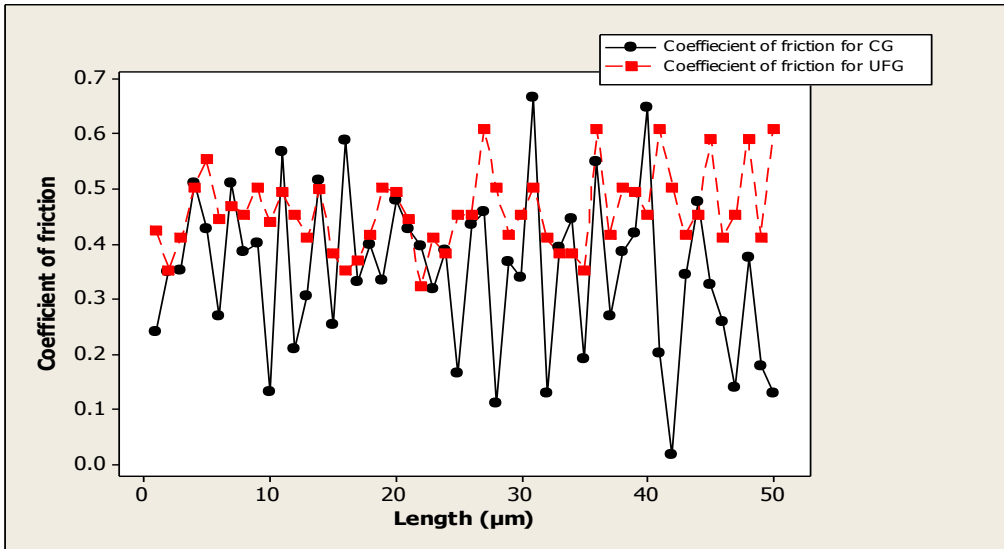


Fig.5: Variation of the coefficient of friction over the AFM measurement range

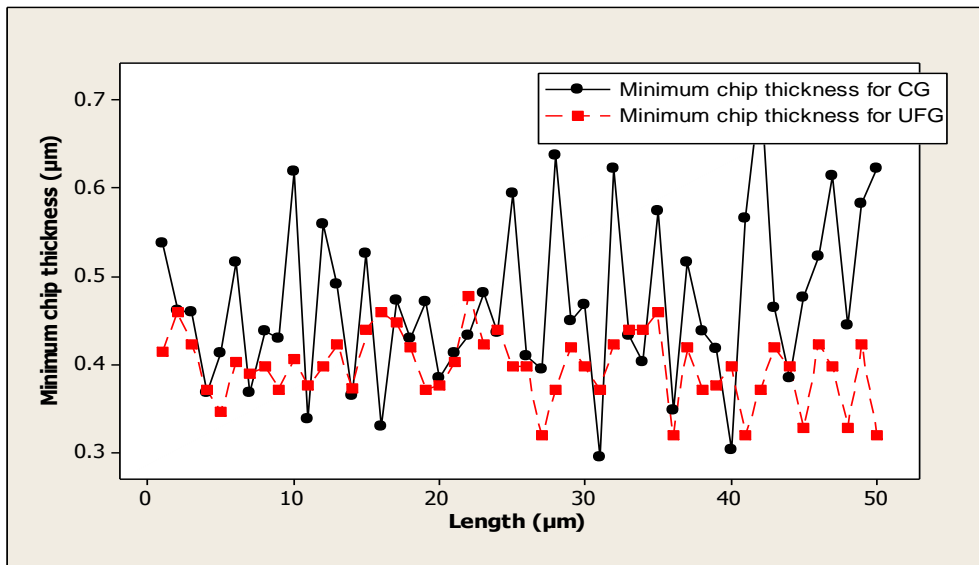
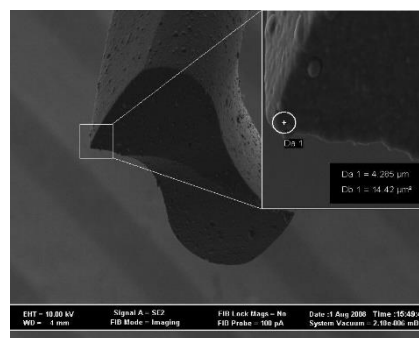


Fig. 6: Minimum chip thickness variations over the AFM measuring range

### 3.3 Micro-milling tests

The machining response of CG and UFG Cu was investigated by carrying out slotting tests on a Kern HSPC 2216 micro-machining centre [43]. The polymer concrete

mono-block frame of this centre absorbs high frequency vibrations much better than cast iron frames [20], which is very important in micro-milling. Fine grained tungsten carbide tools coated with TiAlN were used in the machining trials. In particular, 200  $\mu\text{m}$  diameter end-mill cutters with two teeth, and  $6^\circ$  rake and  $25^\circ$  helix angles, were utilised in the experiments. Prior to the cutting tests, each cutter was imaged using a scanning electron microscope (SEM) to measure the approximate radii of the cutting edges as shown in Figure 7. It was found that these were in the range 2 to 2.5  $\mu\text{m}$ .



**Fig. 7: SEM image of the cutting edge radius**

Table 1 shows the cutting parameters used in the milling trials. A full factorial experimental design was adopted to study the effects of material microstructure on the resulting surface quality. The undeformed chip thickness was controlled by varying the feed rate per tooth in the slotting operation to achieve values close to the average grain size and in the range of the cutting edge radius.

Cutting speeds were chosen that varied from the maximum available on the machine (40000 rpm) to a low value of 8000 rpm. Only one level of axial depth of cut ( $7 \mu\text{m}$ ) was applied due to the limited effect of these parameters on the surface roughness in micro-milling [43]. Note that each set of cutting conditions tabulated in table 1 was carried out three times in order to prove the validity of the experimental results.

**Table 1 Cutting conditions**

Cutting parameters	Values					
Depth of cut [ $\mu\text{m}$ ]	7					
Cutting speed [m/min]	25	15	5			
Feed rate [ $\mu\text{m}/\text{tooth}$ ]	8	4	2	1	0.75	0.25

#### **4. Results and discussions**

The topography of the machined floor surface of the two workpieces was investigated. In particular, roughness and surface defects were examined to elucidate the relationship between the machining response and the material microstructure under different cutting conditions.

##### **4.1 Surface roughness**

The roughness of the machined surface, at the bottom of the micro-milled slots, was examined using a MicroXAM scanning white light interferometer from Phase Shift Inc [45] with a 40X optical magnification. A  $194.15 \times 155.65 \mu\text{m}$  area was sampled with about  $1 \mu\text{m}$  resolution in the X-Y direction (normal to the optical axis) and sub-nanometer resolution in the Z direction (along the optical axis). In particular, the average surface roughness  $R_a$  was measured at 5 different places along the centre line of each slot.

For both materials the lowest surface roughness was achieved at the highest speed, 40,000 rpm or 25 m/min, for all different settings as shown in Figure 8. The only exception was observed when the highest feed rate,  $8 \mu\text{m}/\text{tooth}$ , and the mid-range

speed, 24,000 rpm or 15 m/min, were used in the trials. Conversely, the highest roughness was measured at the lowest speed, 8,000 rpm or 5 m/min, for all the settings of the feed rate except for 1  $\mu\text{m}/\text{tooth}$  and 2 $\mu\text{m}/\text{tooth}$  for CG and UFG Cu, respectively, when the surface quality was marginally better at the mid-range setting of the cutting speed.

In the case of CG Cu, reducing the feed rate down to values of 1  $\mu\text{m}/\text{tooth}$  led to an improvement in the surface finish. As shown in Figure 8, the roughness started to increase when the feed rate was 0.75  $\mu\text{m}/\text{tooth}$ , which can be explained by the drastic change in the cutting conditions, in particular, ploughing rather than normal cutting. Further reduction in the feed rate to 0.25  $\mu\text{m}/\text{tooth}$  led to an improvement in the surface finish which could be attributed to changes in the cutting conditions to smearing and burnishing.

When the same micro-milling trials were conducted on the UFG Cu sample, a general improvement in the surface finish was observed compared to the CG material. Again, the roughness decreased when the feed rate was reduced. However, this time, the minimum roughness was achieved at a lower feed rate of 0.75  $\mu\text{m}/\text{tooth}$  as shown in Figure 8. Thus, as far as the resulting surface roughness was concerned, there was a shift in the optimal cutting conditions from 1  $\mu\text{m}/\text{tooth}$  for CG to 0.75  $\mu\text{m}/\text{tooth}$  for UFG Cu99.9E. This change was associated with a reduction in the minimum chip thickness from 0.48 for CG Cu to 0.39  $\mu\text{m}$  for UFG Cu. It is worth noting that there was a good agreement between the experimental results and the minimum chip thickness calculated based on the AFM measurement of the coefficient of friction. Also, the cutting process became very stable at feed rates 2-3 times the calculated minimum chip thickness in both the CG and UFG workpieces. The increase in roughness at a feed rate of 0.25  $\mu\text{m}/\text{tooth}$  suggests that the cutting was already performed below the necessary

minimum chip thickness, which led to a change of the cutting conditions from normal cutting to more ploughing.

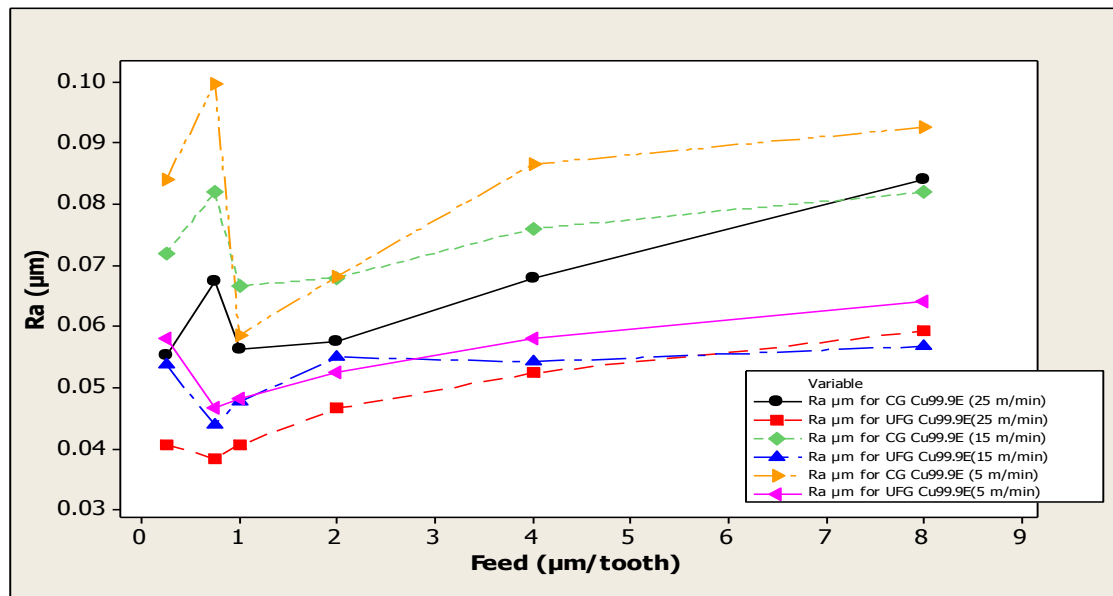


Fig. 8: Roughness achieved under different cutting conditions for CG and UFG Cu99.9E

However, it was reported that an increase in the cutting speed could influence the machining response of a given material in two ways [32]. First, a higher speed will lead to an increase in the cutting temperature, which will have a softening effect on the material. Consequently, the material will tend to be more ductile and hence the minimum chip thickness also increases. Second, at higher speeds, strain hardening effects are also higher due to an increase in the strain and strain rate, which leads to a reduction in the minimum chip thickness. So, the minimum chip thickness is affected by the changing response of the material to variations of the cutting speed.

In both CG and UFG Cu99.9E, as seen in Fig. 8, there is no shift detected in the chip-loads at which the best surfaces were achieved over the cutting speed range. Thus, it can be concluded that the thermal softening and strain hardening effects are equally important and they cancel each other out. One might argue that the range of cutting

speeds used in the experiments is not sufficiently large to observe any differences in the minimum chip thickness of Cu99.9E. However, the enhancement in the surface finish at high cutting speeds can be attributed to improvements in the material behaviour with reduced side flows and elastic recovery [15].

It should be noted that the cutting conditions under which the measurements of the friction coefficient were conducted were different from those used in the experiments. However, this method can be used to assess the relative improvements in materials' homogeneity as a result of microstructure changes, and thus the associated with these reductions of required minimum chip thickness for stable micro machining. On the other hand, to be generally applicable to any material, further experimental studies are required to "calibrate" the predictions of the minimum chip thickness, especially the possible differences in material response between scanning and micro-cutting conditions has to be examined.

Figure 9 shows how the hardness of the machined surface changed with the feed rate for both materials. For CG Cu99.9E, the hardness remained constant at ~105 HV (under a load of 50 g), down to a feed rate of 1  $\mu\text{m}/\text{tooth}$ , and then started to increase rapidly to ~230 HV when the feed rate was reduced to 0.25  $\mu\text{m}/\text{tooth}$ . This indicates an increase in the work hardening induced at feed rates below 1  $\mu\text{m}/\text{tooth}$  and is associated with changes in the cutting conditions from normal cutting to ploughing at very low feed rates. For UFG Cu99.9E, the constant hardness level was ~125 HV. This level was observed at feed rates down to 0.75  $\mu\text{m}/\text{tooth}$ . There was only a marginal increase in the hardness to ~130 HV at 0.25  $\mu\text{m}/\text{tooth}$ . This again indicates changes in the cutting conditions at feed rates below 0.75  $\mu\text{m}/\text{tooth}$ , from normal cutting to ploughing, but the changes were not as severe as in the case of CG Cu99.9E.

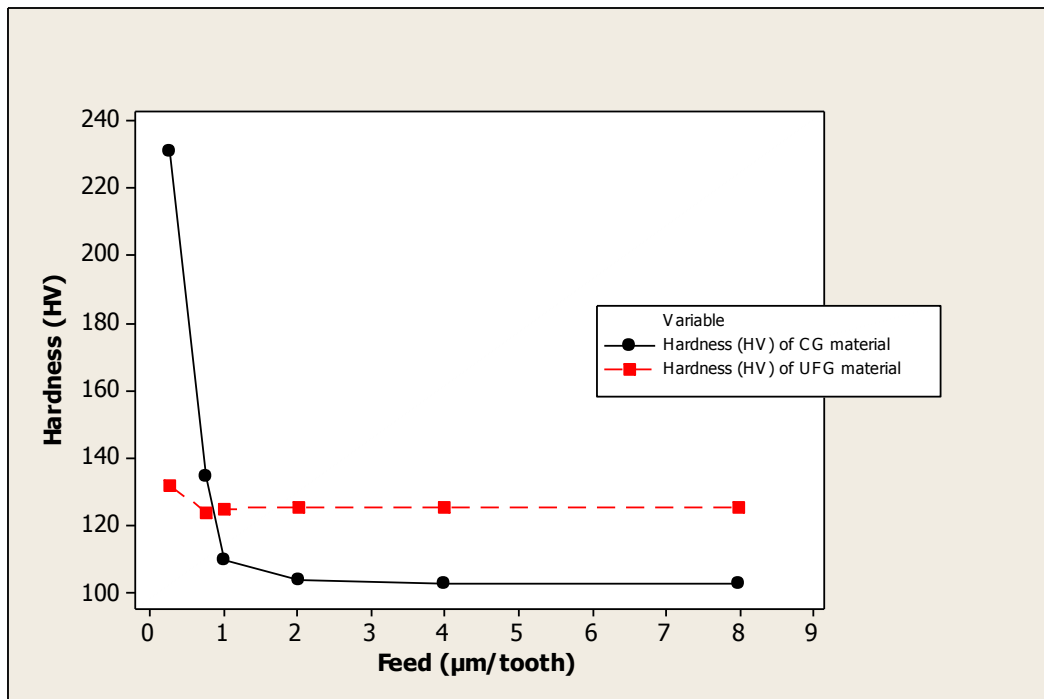


Fig. 9: Hardness of the machined surface

#### 4.2 Surface defects

The surfaces of the machined slots were inspected for defects in a scanning electron microscope. For CG Cu99.9E, as shown in Figure 10, the surface texturing and features observed at a low feed rate of 0.75 µm/tooth were prows (which are severely strain hardened bits of workpiece material), micro-cracks and floor burrs. As noted by other researchers, prows can be the result of a Built-Up Edge (BUE) that has broken off the tool rake face [46]. However, this is not the case in the machining trials conducted by the authors due to the relatively short cutting length. The strain hardening observed on the machined surfaces could be explained by the changes from normal cutting to ploughing at low feed rates due to the cutting edge radius being large compared with the chip-load, and also the relatively high minimum chip thickness required for CG Cu99.9E. In particular, as the chip-load decreased, the cutting tool geometry changed to a negative rake angle and, consequently, cutting was replaced by ploughing. At the

same time, the micro-cracks and the floor burrs could be attributed to the heterogeneity of the material microstructure at the grain level (see Figure 10) which led to changes in mechanical and metallurgical properties at the boundaries between individual grains. This material anisotropy led to significant variations in the minimum chip thickness and thus to chip fragmentation and formation of micro defects.

Conversely, in the case of UFG Cu99.9E the prows observed on the slot edges were minimal and only small burrs were formed. The reason for this was likely to be the high material homogeneity in comparison to CG Cu99.9E.

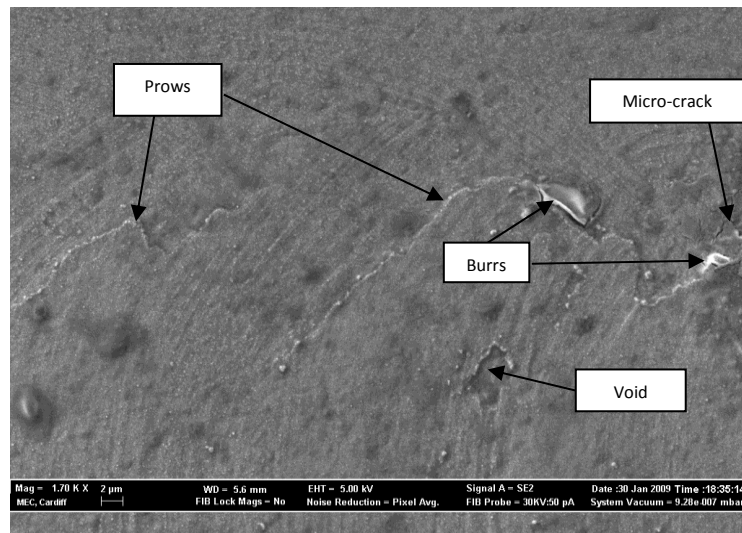


Fig. 10: Machined floor surfaces for CG Cu99.9E at a feed rate of  $0.75 \mu\text{m}/\text{tooth}$  and cutting speed of  $5 \text{ m}/\text{min}$

## 5. Conclusions

Material microstructure effects on micro-milling process, i.e. on cutting conditions and the resulting surface quality, are studied in this paper. An experimental study was conducted to investigate the machining response of two workpieces with different material microstructures. One workpiece was “as received” CG Cu99.9E and the other

was UFG Cu99.9E refined employing the ECAP process. The investigation has shown that through a material microstructure refinement it is possible to improve significantly the cutting conditions in micro-milling and thus to minimise the process scaling down effects in machining micro features. This can lead to a reduction in surface roughness and surface defects which are highly dependent on material homogeneity in micro-cutting. In particular, the following conclusions can be drawn from this investigation:

- For both materials, CG and UFG Cu99.9E, a better surface quality was achieved at high cutting speeds and at feed rates 2 to 3 times higher than the calculated minimum chip thickness. However, a significantly lower surface roughness was achieved at all cutting speeds and feed rates for UFG Cu99.9E compared to the CG material; the best result for the UFG material was  $R_a=0.037$ , while for the CG material it was  $R_a=0.057$ . This constituted a 35% reduction in surface roughness due to the UFG structure. Surface defects such as prows and floor burrs were very pronounced on the CG sample while on the UFG one they were hardly visible as a direct result of the material heterogeneity improvements. Also, there was a shift in the feed rate in achieving the minimum surface roughness from  $1 \mu\text{m/tooth}$  for CG to  $0.75 \mu\text{m/tooth}$  for UFG Cu99.9E, which again could be attributed to the material refinement.
- For CG Cu99.9E, the micro-milled surface hardness achieved was 105 HV and remained constant down to a feed rate of  $1 \mu\text{m/tooth}$ . It started to increase rapidly as the feed rate decreased further. This indicates an increase in work hardening induced at rates below  $1 \mu\text{m/tooth}$ , and suggests changes in the cutting conditions from normal cutting to ploughing at very low feed rates. For UFG Cu99.9E, there

was a hardness increased to 125 HV due to the material refinement, which was 19% higher than for CG Cu99.9E. The hardness increased further at feed rates of 0.75  $\mu\text{m}/\text{tooth}$  and below, which indicates again changes in the cutting conditions, i.e. from cutting to ploughing as a results of the microstructure refinement and UFG Cu99.9E homogeneity improvements.

- An AFM-based method was applied to assess the material homogeneity. It allows the relative homogeneity improvements as a result of the material refinements to be assessed and thus enables the initial setting up of machining parameters. In particular, the method allows the minimum chip thickness to be predicted and thus to have a robust cutting process while minimising the resulting surface roughness. However, it should be noted that in this homogeneity assessment method the cutting conditions in the AFM-based friction coefficient measurements were different from those in micro-milling. At present, this method can be applied to assess relative homogeneity improvements as a result of a material microstructure changes.

### **Acknowledgment**

The research reported in this paper was supported by the FP7 NMP programmes “High Performance Production Line for Small Series Metal Parts” (HYPROLINE, Grant Agreement No 314685) and “High throughput integrated technologies for multi-material functional Micro Components” (HINMICO, Grant Agreement No 609110). Also, the work was carried out within the framework of the EC FP7 CSA project “Advanced Manufacturing of Multi-Material Multi-Functional Products Towards 2020 and Beyond” (4M2020, Grant Agreement 608843).

The authors gratefully acknowledge the support of Prof. M. Richert from AGH University of Science and Technology in Krakow, Poland, who has carried out TEM observations, and Dr. E. Brousseau and Dr. G. Lalev from Cardiff University for their support in inspecting and characterising the machined surfaces and cutting tools.

## Notations

$\beta$	friction angle between a tool and uncut workpiece
$\mu$	coefficient of friction
$\lambda_m$	normalised minimum chip thickness
$L$	length of the cantilever
$l$	vertical distance between the tip of the cantilever and point P (the fixed point of the cantilever)
$r$	cutting tool edge radius
$t_{Cmin}$	minimum chip thickness
$W$	applied force between the tip and the sample; $W$ ranges from 10 to 200 nN;
$\Delta W_1$	absolute values of changes in the normal force when the sample is travelling forward along the direction of the cantilever length
$\Delta W_2$	absolute values of changes in the normal force when the sample is travelling backward along the direction of the cantilever length

## References

1. Liu, X., Devor, R.E., Kapoor, S.G. and Ehmann, K.F., "The Mechanics of Machining at the Microscale: Assessment of the Current State of the Science." *ASME J. of Manufacturing Science and Engineering*, 2004, 126 (4), pp. 666-678.
2. Dhanorker, A., and Özel, T., "Meso/micro scale milling for micro-manufacturing," *Int. J. of Mechatronics and Manufacturing Systems*, 2008, 1(1), pp. 23-42
3. Filiz, S., Conley, C., Wasserman, M., and Ozdoganlar, B., "An experimental investigation of micromachinability of copper 101 using tungsten carbide micro-endmills," *Int. J. of Machine Tools and Manufacture*, 2007, 47, pp. 1088–1100.
4. Chae, J., Park, S.S. and Freiheit, T., "Investigation of Micro-cutting operations," *Int. Journal of Machine Tools and Manufacture*, 2006, 46 (3-4), pp. 313-332.
5. Gowri, S., Kumar, P., Vijayaraj, R., Balan, A.S.S., "Micromachining: technology for the future," *Int. J. of Materials and Structural Integrity*, 2007, 1(1/2/3), pp. 161-179.
6. Gandarias, E., "MICROM: a revolutionary monitoring system to detect tool breakage and collisions, enhance machine cycles and introduce a new probing concept in micro-milling," PhD thesis, Mondragon University, Spain, 2007.
7. Dornfeld, D., Min, S., and Yakeuchi, Y., "Recent advances in mechanical micromachining," *Annals of the CIRP*, 2006, 55 (2), pp. 745-768.
8. Ehmann, K.F., "A synopsis of U.S. micro-manufacturing research and development activities and trends," *Proceedings of the Int. Conf. on Multi-Material Micro Manufacture (4M)*, Borovets, Bulgaria, 2007, pp. 7-13.

9. Pham, D.T., Dimov, S.S., Popov, K.B., Elkaseer, A.M.A., “Effects of microstructure on surface roughness and burr formation in micro-milling: A review,” *Proceedings of 3<sup>rd</sup> Virtual Int. Conf. on Innovative Production Machines and Systems (IPROMS)*, 2008, pp. 270-275.
10. Ng, C., Melkote, S., Rahman, M., and Kumar, A., “Experimental study of micro- and nano-scale cutting of aluminum 7075-T6,” *Int. J. of Machine Tools and Manufacture*, 2006, 46, pp. 929–936.
11. Díaz-Tena, E., Rodríguez-Ezquerro, A., López de Lacalle Marcaide, L.N., Gurtubay Bustinduy L. and Elías Sáenzb, A., “A sustainable process for material removal on pure copper by use of extremophile bacteria,” *Journal of Cleaner Production*, Volume 84, 1 December 2014, Pages 752–760
12. Estíbaliz, D.T., Astrid B., Gorka G., Adrián R., L. Norberto López de Lacalle and Ana E., Biomachining: metal etching via micro-organisms, *Critical Reviews in Biotechnology* 2016, DOI: 10.3109/07388551.2016.1144046
13. Uriarte, L., Azcárate, S., Herrero, A., Lopez de Lacalle, L.N., and Lamikiz, A, “Mechanistic modelling of the micro end milling operation,” *Proceedings of the I MechE Part B, J. of Engineering Manufacture*, 2008, 222 (1), pp. 23-33.
14. Taniguchi, N., (ed), “Nanotechnology: Integrated Processing Systems for Ultra-precision and Ultra-fine Products,” *Oxford University Press*, 1996, ISBN 0 19 8562837.
15. Liu, K., and Melkote, S N., “Effect of plastic side flow on surface roughness in micro-turning process,” *Int. J. of Machine Tools and Manufacture*, 2006, 46(14), pp. 1778-1785.

16. Vogler, M., Kapoor, S. and Devor, R., "On the modeling and analysis of machining performance in microendmilling, Part 1: Surface generation," *ASME J. of Manufacturing Science and Engineering*, 2004, 126, pp. 685–694.
17. Jiao, F., and Cheng, K., "An experimental investigation on micro-milling of polymethyl methacrylate components with nanometric surface roughness," *Proceedings of the Institution of Mechanical Engineers, Part B: Journal of Engineering Manufacture* 0954405413507251, first published on November 1, 2013 doi: 10.1177/0954405413507251)
18. Llanos, I., Agirre, A., Urreta, H., Thepsonthi T., and Ozel, T., "Micromilling high aspect ratio features using tungsten carbide tools" *Proceedings of the Institution of Mechanical Engineers, Part B: Journal of Engineering Manufacture* 0954405414522214, first published on February 25, 2014 doi:10.1177/0954405414522214
19. Kuram, E., and Ozcelik, B., "Optimization of machining parameters during micro-milling of Ti6Al4V titanium alloy and Inconel 718 materials using Taguchi method," *Proceedings of the Institution of Mechanical Engineers, Part B: Journal of Engineering Manufacture* 0954405415572662, first published on February 27, 2015 doi:10.1177/0954405415572662
20. Furukawa, Y, and Moronuki, N., "Effect of material properties on ultra precise cutting processes," *Annals of the CIRP*, 1988, 37 (1), pp. 113-116.
21. Uhlmann, E., Piltz, S., and Schauer, K., "Micro milling of sintered tungsten–copper composite materials," *J. of Materials Processing Technology*, 2005, 167, pp. 402–407.

22. Popov, K.B., Dimov, S.S., Pham, D.T., Minev, R.M., Rosochowski, A., and Olejnik, L., "Micro-milling: material microstructure effects," Proceedings of the I MechE Part B J. of Engineering Manufacture, 220, 2006, pp. 1807-1813.
23. Min, S., Lee, D-E., De Grave, A., Oliveira C.M., J Lin, and Dornfeld, D.A., Surface and Edge Quality Variation in Precision Machining of Single Crystal and Polycrystalline Materials Proceedings of the Institution of Mechanical Engineers, Part B: Journal of Engineering Manufacture April 1, 2006 220: 479-487, doi:10.1243/095440506X77599
24. Mian, A, Mativenga, P T., "Micromachining of coarse grained multi-phase material". Proceedings of the IMechE Part B, J. of Engineering Manufacture, 223 (4), 2009, pp. 377-385. DOI: 10.1243/09544054JEM1185.
25. Mian, A., Driver, N., Mativenga, P. T., "A comparative study of material phase effects on micro-machinability of multiphase materials". Int. J. of Advanced Manufacturing Technology, 50(1-4), 2010, pp. 163-174. DOI: 10.1007/s00170-009-2506-9.
26. Bajpai, V., Salhotra, G., and Singh, R.K., "Micromachining characterization of anisotropic pyrolytic carbon," Proceedings of the Institution of Mechanical Engineers, Part B: Journal of Engineering Manufacture 2041297510393655, first published on August 17, 2011 doi:10.1177/2041297510393655
27. Elkaseer A.M., Dimov S.S., Popov K.B., Negm M. and Minev R., 2012 " Modeling the Material Microstructure Effects on the Surface Generation Process in Microendmilling of Dual-Phase Materials," journal of Manufacturing Science and Engineering, 134, pp. 044501(1-10)

28. Elkaseer, A M A and Brousseau, E.B., 2014, "Modelling the surface generation process during AFM probe-based machining: simulation and experimental validation," *Surf. Topogr.:Metrol. Prop.*, 2025001 (12pp)
29. Lauro, C., Brandão, L., Filho, S., and Baldoc, D., "Analysis of the Forces in Micromilling of Hardened AISI H13 Steel with Different Grain Sizes Using the Taguchi Methodology," *Advances in Mechanical Engineering* January-December 2014 6: 465178, first published on May 8, 2014 doi:10.1155/2014/465178
30. Lauro, C., Filho, S., Baldoc, D., Cerqueira, S., and Brandão, L., "Optimization of micro milling of hardened steel with different grain sizes using multi-objective evolutionary algorithm," *Measurement* 85 (2016) 88–99
31. Choong, Z., Huo, D., Degenaar, P, and O'Neill, A., "Effect of crystallographic orientation and employment of different cutting tools on micro-end-milling of monocrystalline silicon," *Proceedings of the Institution of Mechanical Engineers, Part B: Journal of Engineering Manufacture* 0954405415612379, first published on January 27, 2016 doi:10.1177/0954405415612379
32. Liu, X., Devore, R.E, Kapoor, S.G. "An analytical model for the prediction of minimum chip thickness in micromachining," *ASME J. of Manufacturing Science and Engineering*, 2006, 128, pp. 474-481.
33. Son, S.M., Lim, H.S., and Ahn, J.H., "Effects of friction coefficient on the minimum cutting thickness in micro cutting," *Int. J. Machine Tools and Manufacture*, 2005, 45, pp. 529-535.
34. Mian, A.J., Driver, N., and Mativenga, P.T., "Estimation of minimum chip thickness in micro-milling using acoustic emission," *Proceedings of the Institution of Mechanical Engineers, Part B: Journal of Engineering Manufacture* September 2011 225: 1535-1551, doi:10.1177/0954405411404801

35. Kang, I.S., Kim, J.S., and Seo, Y.W., "Investigation of cutting force behaviour considering the effect of cutting edge radius in the micro-scale milling of AISI 1045 steel," *Proceedings of the Institution of Mechanical Engineers, Part B: Journal of Engineering Manufacture* February 1, 2011 225: 163-171, doi:10.1243/09544054JEM1762
36. Jaffery, S., Khan, M., Ali, L., and Mativenga, P., "Statistical analysis of process parameters in micromachining of Ti-6Al-4V alloy," *Proceedings of the Institution of Mechanical Engineers, Part B: Journal of Engineering Manufacture* 0954405414564409, first published on January 27, 2015 doi:10.1177/0954405414564409
37. Olivera, F., Rodrigues, A., Coelho, R., and Souza, A., "Size effect and minimum chip thickness in micromilling," *International Journal of Machine Tools & Manufacture* 89 (2015) 39–54
38. He, C.L., Zong, W.J., and Sun, T., "Origins for the size effect of surface roughness in diamond turning," *International Journal of Machine Tools & Manufacture* 106 (2016) 22–42
39. Willert, M., Riemer, Brinksmeier, E., "Size effect in micro machining of steel depending on the material state," 7th HPC 2016 – CIRP Conference on High Performance Cutting, *Procedia CIRP* 46 ( 2016 ) 193 – 196
40. Wang, J., Gong, Y., Abba, G., Chen, K., Shi, J. and Cai, G., "Surface generation analysis in micro end milling considering the influences of grain," *Proceedings of Design, Test, Integration and Packaging for MEMS/MOEMS Conference, Stresa, Italy, 2007.*

41. Bhushan, B., "Nananotribology and nanomechanics: An introduction," Online book, URL: [http://books.google.co.uk/books?id=Pi\\_gTu9gnvYC](http://books.google.co.uk/books?id=Pi_gTu9gnvYC), 2005, Last visited: 19 December 2015.
42. Park Systems Corp., URL: [www.parkafm.com](http://www.parkafm.com), 2010, Last visited: 20 December 2015.
43. Kern Machine Tools, Inc. URL: <http://www.kernmachine.com>, 2011, Last visited: 10 January 2016.
44. Wang, W., Kweon, S.H., and Yang, S.H., "A study on roughness of the micro end milled surface produced by a miniaturized machine tool," *J. of Materials Processing Technology*, 2005, 162-163, pp. 702-708.
45. ADE Phase Shift. URL: [www.phase-shift.com](http://www.phase-shift.com), 2010, Last visited: 26 December 2015.
46. Simoneau, A., Ng, E. and Elbestawi, M.A., "Surface defects during microcutting." *Int. J. of Machine Tools and Manufacture*, 2006, 46, pp. 1378–1387.

### **List of figure captions**

Fig. 1: (a) Macro and (b) micro cutting, showing relative dimensions of cutting tool and grain size

Fig 2: Burr size when (a) down-milling and (b) up-milling [25]

Fig. 3: Microstructure of CG (a) and UFG (b, c) Cu99.9E

Fig. 4: Friction force in AFM parallel scan

Fig.5: Variation of the coefficient of friction over the AFM measurement range

Fig. 6: Minimum chip thickness variations over the AFM measuring range

Fig. 7: SEM image of the cutting edge radius

Fig. 8: Roughness achieved under different cutting conditions for CG and UFG Cu99.9E

Fig. 9: Hardness of the machined surface

Fig. 10: Machined floor surfaces for CG Cu99.9E at a feed rate of 0.75  $\mu\text{m}/\text{tooth}$  and cutting speed of 5 m/min